Band-structure and cluster-model calculations of $LaCoO_3$ in the low-spin phase

M. Abbate
Solid State Spectroscopy, University of Nijmegen, Toernooiveld, 6525 ED Nijmegen, The Netherlands

R. Potze and G. A. Sawatzky
Materials Science Centre, University of Groningen, Nijenborgh 18, 9747 AG Groningen, The Netherlands

A. Fujimori
Department of Physics, University of Tokyo, 7-3-1 Hongo, Bunkyo-ku, Tokyo 113, Japan
(Received 13 October 1993)

We present band-structure and cluster-model calculations of $LaCoO_3$ in the low-spin phase. The purpose of these calculations is to contrast and complement the results and conclusions of recent spectroscopic studies. The total density of states (DOS) is compared to the photoemission spectrum; the agreement is very good except for the many-body satellites which appear at higher binding energies. The unoccupied O p DOS reproduces fairly well the O 1s x-ray-absorption spectrum; the main discrepancy appears in the Co 3d region and is attributed to core-hole effects. The ground state predicted by the cluster-model calculation is highly covalent and contains mainly 62% of $t_{2g}^6(^1A_1)$ and 36% of $t_{2g}^6 e_g(^2E)\underline{L}$. The first (one-electron) removal state has more $3d^6\underline{L}$ than $3d^5$ character whereas the first addition state is almost completely dominated by the $3d^7$ state. This means that low-spin $LaCoO_3$ is in the charge-transfer regime and the optical band gap is of the p-d type. The Co 3d contribution to the photoemission spectrum calculated with the cluster-model reproduces not only the leading peaks but also the many-body satellites. The main drawback in this case is the absence of the spectral weight coming from the O 2p bands.

I. INTRODUCTION

The purpose of this paper is to present band-structure and cluster-model calculations of $LaCoO_3$ in the low-spin phase. This compound has attracted much attention in the past because it shows fascinating changes in the electric and magnetic properties as a function of temperature.[1] Recent x-ray and electron spectroscopy studies have helped to elucidate some aspects of its electronic structure.[2–4] But there is a real need to contrast and complement these experimental findings with theoretical calculations. We show below that a combination of band-structure and cluster-model calculations confirm the conclusions of these works and provide a deeper insight into the electronic structure of this material.

The electric and magnetic properties of $LaCoO_3$ present several anomalies around 500 K.[5–9] These anomalies include not only the low-spin to high-spin transition but also a broad semiconductor to metal transition.[10] The latest spectroscopic results indicate that the material is in a low-spin state at low temperatures and the high-spin component increases in the interval 400–650 K.[4] In the following, we concentrate mainly on the electronic structure of $LaCoO_3$ in the low-spin phase. We hope that the results of this study could be the basis for a future attempt to understand the microscopic origin of the spin-state transition.

Band-structure calculations have long provided some of the basic information needed for an understanding of the electronic structure of solids. They offer a good description of ground-state properties such as the total energy and the electronic density. In addition, they do not require adjustable parameters and provide a good treatment of the translational symmetry of the solid. However, this independent-particle approach cannot predict the excitation spectra of narrow-band materials.[11] For instance, band-structure calculations of transition-metal oxides disagree with the magnitude of the experimental band gaps.[12–15]

The failure of the band-structure approach in the prediction of the excitation spectra of narrow-band systems prompted the development of alternative calculation methods.[11] These methods are often based on model Hamiltonians and taken into account the multiplet splitting caused by Coulomb and exchange interactions. For instance, the cluster-model approach provides a good description of the excitation spectra and treats many-body effects explicitly.[16–19] However, this method requires adjustable parameters and neglect completely the dispersion of the bands in the solid.

This survey shows that neither band-structure calculations nor the cluster-model method can be expected to describe correctly all the electronic properties of $LaCoO_3$. However, if both method are used in combination they provide complementary information and the good points of one method compensate, to a certain extent, for the bad points of the other. In addition, we note that the band-structure calculations are expected to be particularly reasonable in this case because low-spin $LaCoO_3$, with a t_{2g}^6 configuration, is a pseudo-closed-shell

 ©1994 The American Physical Society

system. We also note that the parameters used in the cluster-model calculation are not completely arbitrary and follow the expected chemical trends.

II. CALCULATION DETAILS

A. Band-structure calculation

The band structure was calculated within the local-density approximation (LDA) of the density-functional theory.[20,21] The exchange and correlation term was approximated by the formula of Hedin and Lundqvist.[22] The calculation scheme is based on the localized-spherical-wave method,[23] which applies the idea of most-localized orbital to the well-known augmented-spherical-wave method.[24] The program includes an extended basis set to improve the description of the electron bands far above the Fermi level.[25] The same method was used recently to study the electronic structure of the related $LiCoO_2$ compound.[26]

The input of the calculation consists of crystallographic data and a suitable choice of the radius for each atomic sphere. The former can be readily found in the literature, $LaCoO_3$ has a pseudocubic perovskite structure with a rhombohedral distortion along the (111) direction.[27] The space group determined by a best fit to neutron diffraction data is $R\bar{3}c$ and the lattice parameters are $a=5.3778$ Å and $\alpha=60.798$.[28] The unit cell contains two formula units; the ionic positions are given in Table I.

The choice of the radius for each atomic spheres is neither unique nor trivial. We found out that the total density of states (DOS) is rather insensitive to the choice of the radius. This is reasonable since the total DOS should not depend on how the space is divided. By contrast, the electronic charge projected on a given site depends slightly on the size of the spheres. We known by experience that the most sensible results are obtained by using an average of the ionic and atomic radius which are listed in Table I.

The self-consistent potential was determined by iteration on 32 **k** points of the irreducible part of the Brillouin zone (IBZ). We contemplated only nonmagnetic solutions because in this work we are interested mainly in the low-spin ($S=0$) phase. The calculation of the potential included the contribution of both the core electrons and the valence electrons. Finally, the DOS was calculated using a linear tetrahedral technique on 189 **k** points of the IBZ.

TABLE I. Wyckoff labels, ionic positions (with $x=0.2003$), ionic radius, and atomic radius used in the band-structure calculation of $LaCoO_3$ (all radius are given in angstroms).

Element	Wyckoff label	Ionic position	Ionic radius	Atomic radius
La	(2a)	$(\frac{1}{4},\frac{1}{4},\frac{1}{4})$	1.02	1.95
Co	(2b)	(0,0,0)	0.63	1.35
O	(6e)	$(x,\frac{1}{2}-x,\frac{3}{4})$	1.40	0.66

B. Cluster-model calculation

The cluster considered in the present calculation consists of a cobalt ion surrounded by an oxygen octahedra. The lanthanum ions are assumed to be fully ionized and do not contribute to the calculation. The cluster model is solved by the configuration-interaction method which includes various relevant many-body effects. The basis functions are ionic configurations with a well-defined symmetry and include the possibility of multiple charge transfer from the ligands to the metal ion. The ground state can be expanded as

$$|\Phi_{GS}\rangle=\alpha|3d^6\rangle+\beta|3d^7\underline{L}\rangle+\gamma|3d^8\underline{L}^2\rangle\ , \tag{1}$$

where $3d^n$ corresponds to the metal configuration and $\underline{L}$ denotes a ligand hole. Higher-energy configurations are neglected because they have very small occupancies. The basis functions used in the calculation of the ground state are listed in Table II.

The average energy of each term is determined by the values of the charge-transfer energy Δ and the Mott-Hubbard repulsion U.[29] The term splitting caused by Coulomb and exchange interactions as well as crystal-field effects is considered explicitly. The electrostatic interactions are calculated in terms of the Raccah parameters (A, B, and C) and the ionic contribution to the crystal field in terms of $10Dq$.[30] The hybridization among the different configurations is given by the corresponding transfer integral T.[29] The transfer of an e_g (t_{2g}) electron, which forms σ bonds (π bonds), is related to T_σ (T_π). In turn, the transfer integrals can be written in terms of the Slater-Koster parameters $(pd\sigma)$ and $(pd\pi)$.[31,32] In the present calculation, the transfer integrals are determined solely by $(pd\sigma)$ because we assume that $T_\pi\approx -T_\sigma/2$. The matrix elements of the Hamiltonian in the ground state as well as the relationship between the different parameters are given in Table II.

TABLE II. Basis functions, matrix elements, and parameters used in the cluster-model calculation of the ground state [where $\underline{t}(\underline{e})$ denotes a ligand hole of $t_{2g}(e_g)$ symmetry].

Basic functions	Diagonal matrix elements	Off-diagonal	Parameters
$\|1\rangle=\|t_{2g}^6(^1A_1)\rangle$	$H_{1,1}=15A-30B+15C-E(d^6)-24Dq$	$H_{1,2}=2T_\sigma$	$T_\sigma=\sqrt{(3)}(pd\sigma)$
$\|2\rangle=\|t_{2g}^6e_g(^2E)\underline{e}\rangle$	$H_{2,2}=21A-36B+18C-E(d^7)-18Dq+\Delta$	$H_{2,3}=\sqrt{\frac{3}{2}}T_\sigma$	$T_\pi\approx -T_\sigma/2$
$\|3\rangle=\|t_{2g}^6e_g^2(^3A_2)\underline{e}^2\rangle$	$H_{3,3}=28A-50B+21C-E(d^8)-12Dq+2\Delta+U$	$H_{2,4}=\sqrt{\frac{1}{2}}T_\sigma$	$E(d^n)=\frac{1}{2}n(n-1)U$
$\|4\rangle=\|t_{2g}^6e_g^2(^1A_1)\underline{e}^2\rangle$	$H_{4,4}=28A-34B+25C-E(d^8)-12Dq+2\Delta+U$	$H_{2,5}=-T_\sigma$	$U=A-\frac{14}{9}B+\frac{7}{9}C$
$\|5\rangle=\|t_{2g}^6e_g^2(^1E)\underline{e}^2\rangle$	$H_{5,5}=28A-42B+23C-E(d^8)-12Dq+2\Delta+U$		

TABLE III. Basis functions used in the cluster-model calculation of the final state [where $\underline{t}(\underline{e})$ denotes a ligand hole of $t_{2g}(e_g)$ symmetry].

Final-state functions				
$\lvert t_{2g}^5(^2T_2)\rangle$	$\lvert t_{2g}^6(^1A_1)\underline{t}\rangle$	$\lvert t_{2g}^5 e_g(^3T_1)\underline{e}\rangle$	$\lvert t_{2g}^5 e_g(^3T_2)\underline{e}\rangle$	$\lvert t_{2g}^5 e_g(^1T_1)\underline{e}\rangle$
$\lvert t_{2g}^5 e_g(^1T_2)\underline{e}\rangle$	$\lvert t_{2g}^6 e_g(^2E)\underline{t}\,\underline{e}\rangle$	$\lvert t_{2g}^5 e_g^2(^4T_1)\underline{e}^2\rangle$	$\lvert t_{2g}^5 e_g^2(^2T_1)\underline{e}^2\rangle$	$\lvert t_{2g}^5 e_g^2(^2T_2)\underline{e}^2\rangle$

The metal-d contribution to the photoemission spectra was calculated using the sudden approximation

$$I(E)=\sum |\langle \Phi_f|d|\Phi_{\rm GS}\rangle|^2\delta(E-E_f+E_{\rm GS})\ , \qquad (2)$$

where the d operator annihilates a metal-d electron and the sum extends to all possible final states $|\Phi_f\rangle$. The final states can be expanded as

$$|\Phi_f\rangle=a_f|3d^5\rangle+b_f|3d^6\underline{L}\rangle+c_f|3d^7\underline{L}^2\rangle\ , \qquad (3)$$

where the subindex f labels different final states. The basis functions used in this calculation are listed in Table III; the matrix elements of the Hamiltonian in this case are omitted for brevity. The formula for the photoemission spectra can then be written as

$$I(E)=\sum |\alpha a_f A_f+\beta b_f B_f+\gamma c_f C_f|^2\delta(E-E_f+E_{\rm GS})\ , \qquad (4)$$

where A_f, B_f, and C_f are the appropriate transition matrix elements. The calculation of these matrix elements in systems with several open shells involves not only the corresponding fractional parentage coefficient but also the necessary coupling coefficients.[33,34] The coefficient of fractional parentage can be found in Ref. 35, the orbital Raccah W coefficients are given in Ref. 36, and the spin Raccah W coefficients are listed in Ref. 37. The relative matrix elements of the most relevant transition channels are given in Table IV.

III. RESULTS AND DISCUSSION

A. Band-structure calculation

Figure 1 shows the total DOS of $LaCoO_3$ projected on the different atomic sites.[38] We stress again that these DOS results correspond to a nonmagnetic solution because we are interested only in the low-spin ($S=0$) state.

TABLE IV. Relative transition matrix elements between the different basis functions used in the cluster-model calculation of the ground state and the final state [where $\underline{t}(\underline{e})$ denotes a ligand hole of $t_{2g}(e_g)$ symmetry]. Only the most relevant ionization channels are shown here.

Transition matrix elements
$\langle t_{2g}^5(^2T_2)\lvert d\rvert t_{2g}^6(^1A_1)\rangle=\sqrt{6}$
$\langle t_{2g}^6(^1A_1)\underline{t}\lvert d\rvert t_{2g}^6 e_g(^2E)\underline{e}\rangle=0$
$\langle t_{2g}^5 e_g(^3T_1)\underline{e}\lvert d\rvert t_{2g}^6 e_g(^2E)\underline{e}\rangle=-\frac{3}{2}$
$\langle t_{2g}^5 e_g(^3T_2)\underline{e}\lvert d\rvert t_{2g}^6 e_g(^2E)\underline{e}\rangle=\frac{3}{2}$
$\langle t_{2g}^5 e_g(^1T_1)\underline{e}\lvert d\rvert t_{2g}^6 e_g(^2E)\underline{e}\rangle=\sqrt{3}/2$
$\langle t_{2g}^5 e_g(^1T_2)\underline{e}\lvert d\rvert t_{2g}^6 e_g(^2E)\underline{e}\rangle=-\sqrt{3}/2$

First of all, the results predicts a metallic behavior for $LaCoO_3$ because the total DOS is continuous at the Fermi energy, although it has a sharp minimum at E_F. This is in contrast with the semiconducting behavior observed for $LaCoO_3$ in the low-spin phase.[39,40] As mentioned above, this kind of discrepancy can be expected in narrow-band materials and shows clearly the limitations of the band-structure approach.[41] Second, the total DOS presents rather sharp features in the valence band and, except for the sharp band at 4 eV, a relatively smoother structure in the conduction band. The O and Co spectral weights are heavily mixed and appear concentrated mainly in the valence band. By contrast, the La spectral weight contributes mainly to the unoccupied electronic states in the conduction band. This suggests that La presents a more ionic character stabilized by the Madelung potential while the covalent contribution to the bonding is much larger within the Co-O octahedra. These conclusions are in agreement with intuitive chemical ideas.

The partial DOS for each element projected on the different orbital quantum numbers are shown in Figs. 2–4. First of all, La contributes with small amounts of $6sp$ and $5d$ character to the valence band. However, most of the La character remains unoccupied and appears spread in the conduction band. In particular, the sharp

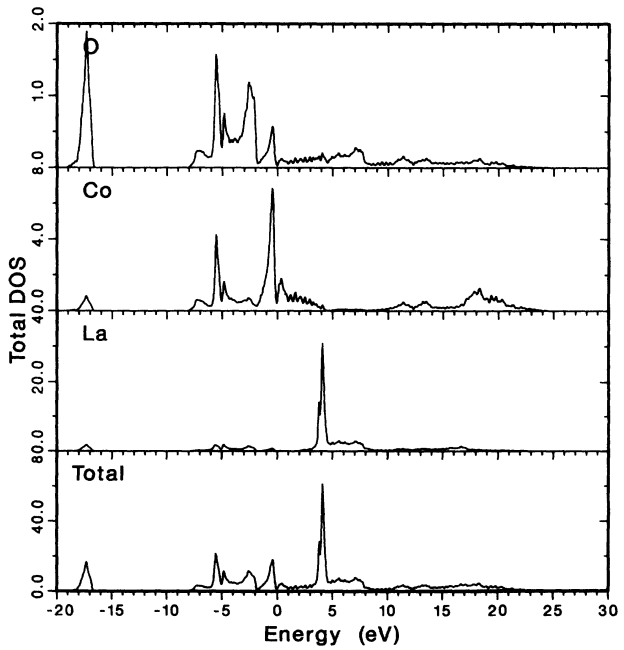

FIG. 1. Total density of states (DOS) of $LaCoO_3$ projected on the different atomic sites (states/eV).

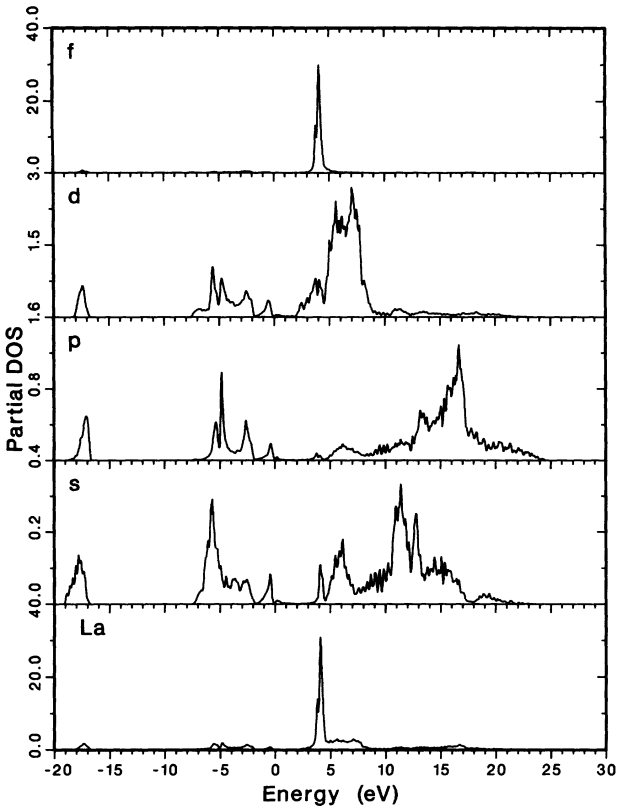

FIG. 2. Partial DOS of $LaCoO_3$ at the La site projected on the different orbital quantum numbers (states/eV).

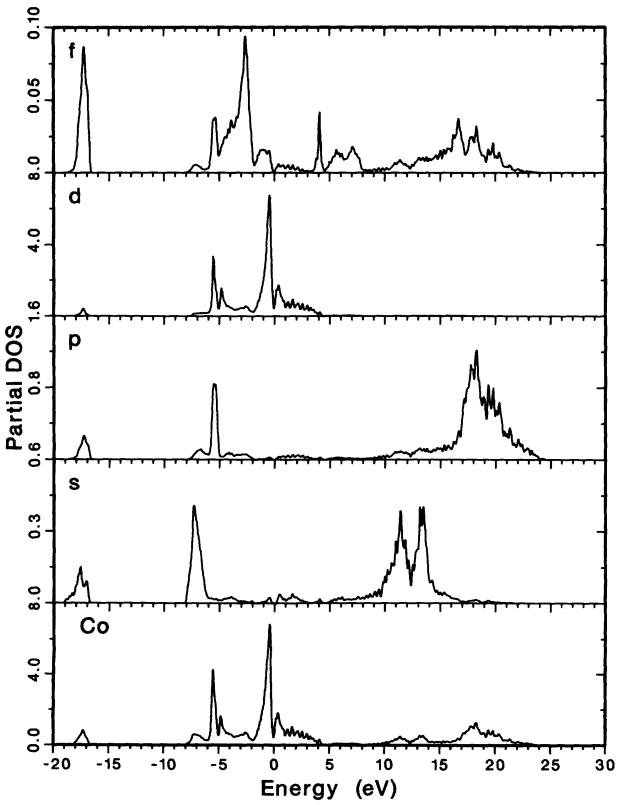

FIG. 3. Partial DOS of $LaCoO_3$ at the Co site projected on the different orbital quantum numbers (states/eV).

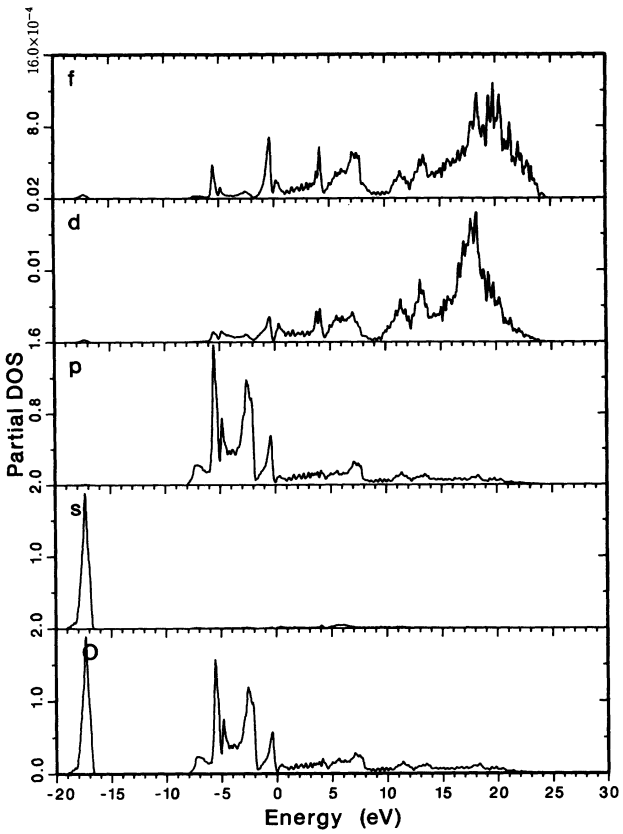

FIG. 4. Partial DOS of $LaCoO_3$ at the O site projected on the different orbital quantum numbers (states/eV).

feature at 4 eV above the Fermi level corresponds to the La $4f$ band, the band at 4–8 eV is composed mainly of La $5d$ states, and the La $6sp$ states contribute mainly in the 10–20 eV region. The Co $3d$ states contributes very strongly to the valence band and to the first 4 eV in the conduction band. By contrast, the Co $4s$ and $4p$ characters are present, respectively, in the 10–15 and 15–20 eV regions of the conduction band. Finally, the O $2s$ states form the sharp band at 17–18 eV below the Fermi level while the O $2p$ states present strong features throughout the valence band. These results suggest a strong covalent bonding between the O $2p$ and Co $3d$ states and almost complete ionization of the Co $4sp$ and the La $6sp$ electrons. In turn, this supports the assumption made above that only the Co $3d$ and the O $2p$ electrons should be considered in the cluster-model calculation.

The Co $3d$ states are very important and deserve to be discussed in more detail because they determine the electronic properties of $LaCoO_3$. First of all, the strong peak below the Fermi level corresponds to the Co t_{2g} bands. These relatively nonbonding states produce weak Co-O-Co interactions which give rise to a narrow band. By contrast, the Co e_g states produce very strong Co-O-Co interactions which give rise to a much larger dispersion and results in the broader e_g band observed just above the Fermi level. Finally, the Co $3d$ spectral weight at the bottom of the valence band is mixed in states which have mainly O $2p$ character. This mixing provides a direct indication of the covalent contribution to the Co $3d$–O $2p$

bonding. We note that the overall picture is *consistent* with a low-spin state where the t_{2g} band is completely filled and gives rise to a t_{2g}^6 configuration, while the e_g band remains completely empty.

The Co 3*d* bands presents some similarities with those observed in the related compound $LiCoO_2$, which also has Co^{3+} ions in a low-spin state.[26] The main differences in the Co 3*d* bands of $LiCoO_2$ are (i) the band gap between the t_{2g} and e_g bands is larger,[42] (ii) the e_g states form a narrower band, and (iii) the Co 3*d*–O 2*p* mixing at the bottom of the valence band is smaller. These differences are caused by a completely different chemical and crystallographic structure which cause changes in the Madelung potential and the Co 3*d*–O 2*p* interactions. The relatively larger separation between the t_{2g} and e_g bands in $LiCoO_2$ is consistent with a well defined and stable low-spin state. By contrast, the smaller separation in $LaCoO_3$ suggests a near instability which is consistent with the observed spin transition. Finally, the much larger Co 3*d*–O 2*p* mixing at the bottom of the valence band in $LaCoO_3$ indicates a more covalent ground state than in $LiCoO_2$.

The results of the band-structure calculation can now be compared to the valence-band and x-ray absorption spectra reported recently.[4] As indicated above, the comparison is feasible because low-spin $LaCoO_3$ is a pseudo-closed-shell system and consequently multiplet effects are expected to be negligible. The band-structure result used in the comparison depends on the experimental technique. For instance, the photoemission spectrum can be related in a first approximation to the total DOS because the total ionization cross section of the Co 3*d* and O 2*p* electrons in this compound (which give the main contribution to the valence-band spectrum) are of the same order (0.4 and 0.2×10^{-2} Mb, respectively).[43] On the other hand, the O 1*s* x-ray absorption spectrum should be compared to the unoccupied O *p* DOS to take into account the local character of the excitation process and the dipole selection rule.[44] The band-structure results were broadened with a Gaussian function to take into account the experimental resolution and with an energy-dependent Lorentzian function to account for the finite lifetime of the final state.[26] In addition, the calculated spectrum was shifted by hand to get the best overall agreement with the experimental result.

Figure 5 compares the photoemission spectrum of $LaCoO_3$ in the low-spin phase taken from Ref. 4 with the total DOS. As expected, the calculated spectrum reproduces quite well the intensity and energy position of all the major peaks. The main discrepancy is the absence of the satellites at 10–12 eV in the calculated spectrum. These satellites are caused by many-body effects which are beyond the capabilities of the band-structure calculation approach. As discussed above, the sharp peak at 1.3 eV corresponds mainly to the Co t_{2g} band. On the other hand, the broader features at 3.5 and 5.5 eV correspond mainly to the O 2*p* bands. It is worth noting here that the O 2*p* character contributes significantly to the spectrum and presents a rich structure in the 3–6 eV region. This means that the *d*-metal contribution to the photoemission spectrum calculated with the cluster-model below cannot be expected to explain all the spectral details in this energy region.

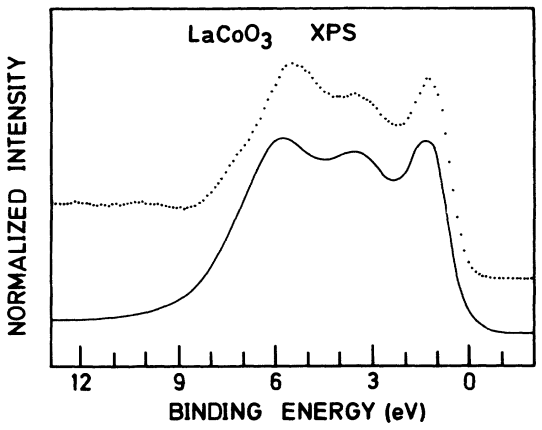

FIG. 5. Comparison between the broadened total DOS (solid line) and the photoemission spectrum of $LaCoO_3$ in the low-spin phase (dots).

Figure 6 compares the O 1*s* x-ray absorption spectrum of $LaCoO_3$ in the low-spin phase taken from Ref. 4 with the unoccupied O *p* DOS. The calculated spectrum reproduces most of the experimental features and the overall agreement is fairly good. The comparison confirms precisely the same qualitative assignments proposed in Ref. 4. In particular, the peak at 530 eV corresponds to the Co e_g band, the bump at 536 eV to the La 5*d* band and the broad structure with two peaks around 539–547 eV to Co 4*sp* and La 6*sp* bands.[45] The main discrepancy appears in the Co 3*d* band region, namely, the experimental result shows a peak skewed towards threshold while the calculated spectrum presents a rather flat band. Grioni *et al.* have shown convincingly that this redistribution of the spectral weight in the transition-metal 3*d* region can be attributed to the influence of the O 1*s* core hole.[46] There are also some minor discrepancies in the peak positions of the La 5*d* and (La+Co) *sp* bands which are attributed to additional self-energy effects.[47]

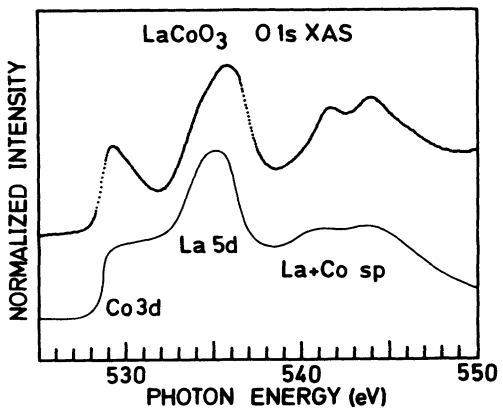

FIG. 6. Comparison between the broadened O *p* partial DOS (solid line) and the O 1*s* x-ray absorption spectrum of $LaCoO_3$ in the low-spin phase (dots).

B. Cluster-model calculation

The cluster-model calculations were performed with the parameter set listed in Table V. Some of these parameters were fixed beforehand while others were treated as adjustable parameters. For instance, the Raccah parameters B and C are hardly affected by the solid-state environment and were set to the free-ion values quoted in Ref. 30. In addition, the ionic contribution to the crystal-field splitting $10Dq$ was set to 1.2 eV; this value was chosen to ensure that the low-spin state were more stable than the high-spin state.[48] By contrast, the other parameters, including Δ, U, and $(pd\sigma)$, depend very strongly on the compound and are very difficult to estimate. It is customary to adjust these parameters to obtain the best agreement with the spectroscopic results. We note that the values of the parameters used in the present calculation are similar to those used in the related $LiCoO_2$ compound[49] and follow the expected chemical trends.[50,51]

The schematic energy level diagram for a low-spin Co^{3+} ion in octahedral symmetry is given in Fig. 7. First of all, the average energy of the different configurations is given in terms of Δ and U, as indicated in Fig. 7(a). We show below that the influence of higher-energy configurations is very small and can be neglected in a first approximation. Next, the term splitting caused by the electrostatic interactions and crystal-field effects is illustrated in Fig. 7(b). These unperturbed energy levels correspond to the basis states used in the present cluster-model calculation. Finally, the different basis states are mixed by the corresponding transfer integrals. The ground state corresponds to the combination with the lowest energy, as shown in Fig. 7(c).

Table VI summarizes the symmetry, spin, and configuration occupancies of the ground state, the first (one-electron) removal state and the first addition state. The ground state is composed mainly of $t_{2g}^6(^1A_1)$ and $t_{2g}^6e_g(^2E)\underline{e}$; the occupancies of these states are 0.62 and 0.36, respectively. The relatively large occupancy of the $3d^7\underline{L}$ state indicates a highly covalent ground state. Table VI shows also that the contribution of higher-energy configurations is very small; the total occupancy of the $3d^8\underline{L}^2$ terms is only 0.02. These occupancies are in good agreement with previous estimates based on a much simpler model.[4] The relative occupancies of the different configurations in the ground state is dictated mainly by the ratio between the hybridization strength $(pd\sigma)$ and the energy difference Δ. The main contributions to the stability of the ground state come from the crystal-field energy of the primary $t_{2g}^6(^1A_1)$ basis state, see Fig. 7(b), and the extra energy lowering caused by the particularly strong hybridization with the $t_{2g}^6e_g(^2E)\underline{e}$ state, see Fig. 7(c).

TABLE V. Parameter set used in the cluster-model calculation (all values are given in eV).

Fixed parameters	Adjustable parameters
$10Dq=1.2$	$U=5.0$
$B=0.13$	$\Delta=4.0$
$C=0.64$	$(pd\sigma)=-1.5$

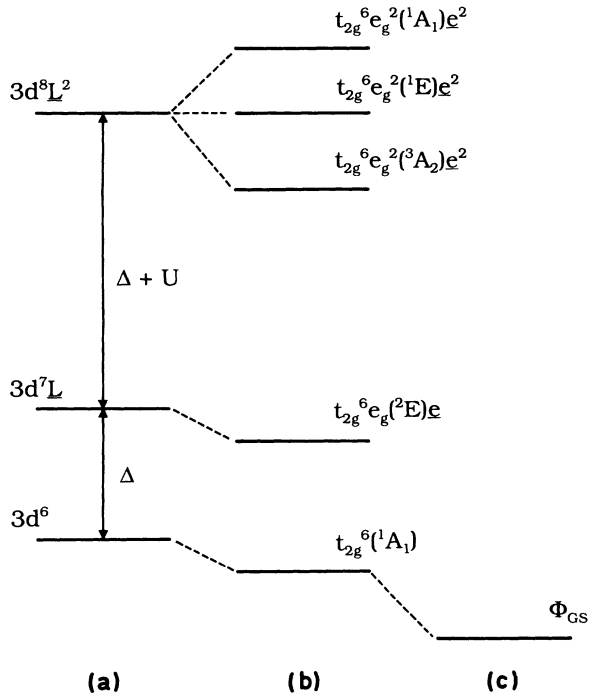

FIG. 7. Approximate energy-level diagram of a low-spin Co^{3+} ion in octahedral symmetry. (a) The average energy of the different configurations is given in terms of Δ and U. (b) The term splitting is caused by electrostatic interactions and crystal-field effects. (c) The hybridization mixes the different basis states and gives rise to a highly covalent ground state.

The character of the first (one-electron) removal states is dictated by the $t_{2g}^5(^2T_2)$ state, which derives from the one-electron removal of the primary $t_{2g}^6(^1A_1)$ term in the ground state. However, the total occupancy of the $3d^6\underline{L}$ terms (approximately 0.57) is much larger than that of the $3d^5$ configuration (around 0.13). This means that the first (one-electron) removal state contains more O $2p$ than Co $3d$ character; this is an important factor in determining the nature of the optical band gap; see below. The relative occupancies in this case are given by the ratio between the hybridization strength $(pd\sigma)$ and the energy difference $(U-\Delta)$. The sign of the energy difference $(U-\Delta)$ is very important because it determines the dominant configuration (either $3d^5$ or $3d^6\underline{L}$) in the first (one-electron) removal state. On the other hand, the symmetry and spin of the first addition state is dictated by the $t_{2g}^6e_g(^2E)$ term which is the result of adding one electron to the primary $t_{2g}^6(^1A_1)$ state. Table VI shows that the first addition state is dominated almost completely by the $3d^7$ configuration with an occupancy of approximately 0.81. The relative population in this case depends on the ratio between the hybridization strength $(pd\sigma)$ and the energy difference $(U+\Delta)$.

We discuss now the nature of the optical band gap of $LaCoO_3$ in the low-spin phase. In particular, we want to know whether $LaCoO_3$ is in the Mott-Hubbard (d-d band gap) or in the charge-transfer (p-d band gap) regime.

TABLE VI. Orbital occupancies of the different configurations in the ground state ($^1A_1$), the first (one-electron) removal state ($^2T_2$), and the first addition state (^2E).

Ground state ($^1A_1$)		Removal state ($^2T_2$)		Addition state (^2E)	
$3d^6$	0.62	$3d^5$	0.13	$3d^7$	0.81
$3d^7\underline{L}$	0.36	$3d^6\underline{L}$	0.57	$3d^8\underline{L}$	0.17
$3d^8\underline{L}^2$	0.02	$3d^7\underline{L}^2$	0.30	$3d^9\underline{L}^2$	0.02

This is determined by the relative values of U and Δ defined with respect to the lowest energy multiplet, as shown by Zaanen, Sawatzky, and Allen.[52] Alternatively, the nature of the optical band gap is given directly by the character of the first (one-electron) removal and the first addition state. In this case, the removal state is dominated by the $3d^6\underline{L}$ terms and the addition state by the $3d^7$ configuration. This means that the optical band gap involves excitation from O $2p$ states to Co $3d$ states and that low-spin $LaCoO_3$ is in the charge-transfer regime. We note that this kind of behavior is to be expected in most late-transition-metal oxides.[53,54] Finally, we want to point out that the optical gap might not coincide with the conductivity gap.[55] In particular, the true first removal state might really derive from the high-spin $t_{2g}^3e_g^2(^6A_1)$ state. This state cannot be reached by a one-electron excitation of the ground state but could be thermally excited in a conductivity experiment.

Figure 8 compares the photoemission spectrum of $LaCoO_3$ in the low-spin phase taken from Ref. 4 and the Co $3d$ removal spectrum calculated with the cluster model. The values of the adjustable parameters used in the cluster-model calculation were tuned according to the following criteria. First, the hybridization strength ($pd\sigma$) was adjusted to give the correct energy spread of the multiplet. Next, the energy difference ($U-\Delta$) was tuned to give the correct distribution of spectral weight among the different features. Finally, the approximate value of the charge-transfer energy Δ was estimated from the energy shift with respect to the experimental spectrum. The calculated spectrum reproduces fairly well the leading peaks and all major features; the main discrepancy is the lack of spectral weight in the 4–6 eV region. The agreement is reasonable if we remember that the O $2p$ contribution to the spectrum appears precisely in this energy region. First of all, the leading peak at 1.3 eV corresponds to the first (one-electron) removal state of $LaCoO_3$. According to the cluster-model calculation this state contains more $3d^6\underline{L}$ than $3d^5$ character while the band-structure calculation predicted wrongly that this peak corresponds mainly to the Co $3d$ band. Next, the peaks at 4 and 6 eV correspond to mixtures of $3d^6\underline{L}$ and $3d^5$ states which were related in the band-structure spectrum to O $2p$ bands mixed with Co $3d$ states. Finally, we note that the cluster-model calculation reproduces also the many-body satellites at higher binding energies which were absent in the band-structure calculation.

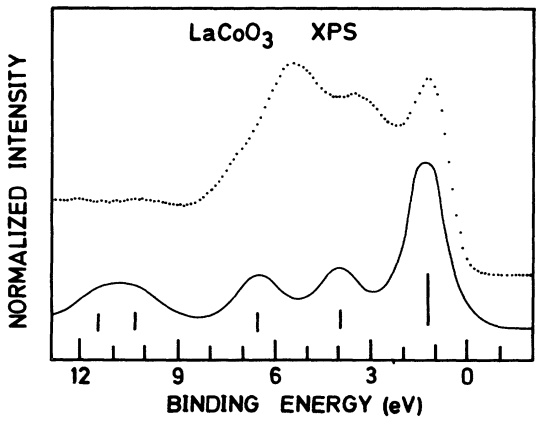

FIG. 8. Comparison between the Co $3d$ removal spectrum calculated with the cluster model (solid line) and the photoemission spectrum of $LaCoO_3$ in the low-spin phase (dots).

It is worth discussing the differences between the independent-particle (band-structure) and the many-body (cluster-model) approaches. In particular, the discrepancy concerning the interpretation of the 1.3 eV peak in the photoemission spectrum. According to the band-structure calculation this band contains mainly Co $3d$ character. This interpretation is wrong because this independent-particle approach neglect electron correlation effects. The correct interpretation in this case is given by the cluster-model calculation which indicates that the peak contains more $3d^6\underline{L}$ than $3d^5$ character. This kind of discrepancy is not just a coincidence, but it is to be expected for all charge-transfer materials such as the late-transition-metal oxides.[16–19] In our previous paper (Ref. 4) we failed to recognize that the 1.3 eV peak contained more O $2p$ than Co $3d$ character. However, even containing more O $2p$ character, this peak is still characteristic of the low-spin state. Therefore, the conclusion in Ref. 4 that the decrease of this peak at higher temperatures is related to the decrease of the low-spin population is still correct.

IV. SUMMARY AND CONCLUSIONS

To summarize, we have presented band-structure and cluster-model calculations of $LaCoO_3$ in the low-spin phase. The band-structure calculation predicts a metallic state for $LaCoO_3$ in the low-spin phase which is at variance with the semiconducting behavior observed experimentally. This discrepancy illustrates once more the limitations of the simple LDA approach to narrow-band materials. The band-structure results suggest a strong covalent bonding between the O $2p$ and Co $3d$ states and almost complete ionization of the Co $4sp$ and La $6sp$ electrons. The total DOS is compared to the valence-band photoemission spectrum; the agreement is very good except for the many-body satellites at higher binding ener-

gies. The unoccupied O p DOS compares reasonably well with the O 1s x-ray absorption spectrum; the main discrepancy appears in the Co 3d region and is attributed to core-hole effects. Finally, the relatively good agreement with the spectroscopic results is due to the fact that low-spin $LaCoO_3$ is a pseudo-closed-shell system.

The cluster-model calculation predicts a highly covalent ground state with 62% of $t_{2g}^6(^1A_1)$ and 36% of $t_{2g}^6e_g(^2E)\underline{e}$. The main contributions to the stability of the ground state are the crystal-field energy of the $t_{2g}^6(^1A_1)$ basis state and the strong hybridization with the $t_{2g}^6e_g(^2E)\underline{e}$ state. The first (one-electron) removal state contains more $3d^6\underline{L}$ than $3d^5$ character whereas the first addition state is almost completely dominated by the $3d^7$ state. This means that low-spin $LaCoO_3$ is in the charge-transfer regime and the optical band-gap is of the p-d type. The Co 3d contribution to the photoemission spectrum calculated with the cluster-model reproduces the leading peaks and the many-body satellites but fails to explain the spectral weight coming from the O 2p bands. Finally, we want to point out that the adjustable parameters used in the cluster-model calculation follow the expected chemical trend.

To conclude, this work illustrates the complementary point of views of band-structure and cluster-model calculations and shows the potential of studies of narrow-band materials based on the combined use of both approaches. Finally, we hope that the results presented here could be the basis for a future attempt to understand the microscopic origin of the spin-state transition in $LaCoO_3$.

ACKNOWLEDGMENTS

We would like to thank John Inglesfield for many useful comments and Rob de Groot and Marek Czyzyk for help with the band-structure calculation. This work was partially supported by Fundamenteel Onderzoek der Materie, Scheikunde Onderzoek Nederland, and the European Community Science program.

[1] J. B. Goodenough, in *Progress in Solid State Chemistry,* edited by H. Reiss (Pergamon, Oxford, 1972), Vol. 5.
[2] D. D. Sarma, A. Chainani, R. Cimino, P. Sen, C. Carbone, M. Mathew, and W. Gudat, Europhys. Lett. **19**, 513 (1992).
[3] A. Chainani, M. Mathew, and D. D. Sarma, Phys. Rev. B **46**, 9976 (1992).
[4] M. Abbate, J. C. Fuggle, A. Fujimori, L. H. Tjeng, C. T. Chen, R. Potze, G. A. Sawatzky, H. Eisaki, and S. Uchida, Phys. Rev. B **47**, 16 124 (1993).
[5] R. R. Heikes, R. C. Miller, and R. Mazelsky, Physica **30**, 1600 (1964).
[6] G. Blasse, J. Appl. Phys. **36**, 879 (1965).
[7] C. S. Naiman, R. Gilmore, B. DiBartolo, A. Linz, and R. Santoro, J. Appl. Phys. **36**, 1044 (1966).
[8] G. H. Jonker, J. Appl. Phys. **37**, 1424 (1966).
[9] N. Menyuk, K. Dwight, and P. M. Raccah, J. Phys. Chem. Solids **28**, 549 (1967).
[10] A thorough survey of the early literature can be found in Ref. 4.
[11] *Narrow Band Phenomena,* edited by J. C. Fuggle, G. A. Sawatzky, and J. W. Allen (Plenum, New York, 1988).
[12] K. Terakura, A. R. Williams, T. Oguchi, and J. Kübler, Phys. Rev. Lett. **52**, 1830 (1984).
[13] K. Terakura, T. Oguchi, A. R. Williams, and J. Kübler, Phys. Rev. B **30**, 4734 (1984).
[14] M. R. Norman, Phys. Rev. B **40**, 10 632 (1989).
[15] M. R. Norman, Phys. Rev. Lett. **64**, 1162 (1990).
[16] A. Fujimori, F. Minami, and S. Sugano, Phys. Rev. B **29**, 5225 (1984).
[17] A. Fujimori and F. Minami, Phys. Rev. B **30**, 957 (1984).
[18] G. A. Sawatzky and J. W. Allen, Phys. Rev. Lett. **53**, 2339 (1984).
[19] S. Hüfner, F. Hulliger, J. Osterwalder, and T. Riesterer, Solid State Commun. **50**, 83 (1984).
[20] P. Hohemberg and W. Kohn, Phys. Rev. **136**, B864 (1964).
[21] W. Kohn and L. J. Sham, Phys. Rev. **140**, A1133 (1965).
[22] L. Hedin and B. I. Lundqvist, J. Phys. C **3**, 2065 (1971).
[23] H. van Leuken, A. Lodder, M. T. Czyzyk, F. Springelkamp, and R. A. de Groot, Phys. Rev. B **41**, 5613 (1990).
[24] A. R. Williams, J. Kübler, and C. D. Gellat, Phys. Rev. B **19**, 6094 (1979).
[25] M. T. Czyzyk, R. A. de Groot, G. Dalba, P. Fornasini, A. Kisiel, F. Rocca, and E. Burattini, Phys. Rev. B **39**, 9831 (1989).
[26] M. T. Czyzyk, R. Potze, and G. A. Sawatzky, Phys. Rev. B **46**, 3729 (1992).
[27] P. M. Raccah and J. B. Goodenough, Phys. Rev. **155**, 932 (1967).
[28] G. Thornton, B. C. Tofield, and A. W. Hewat, J. Solid State Chem. **61**, 301 (1986).
[29] G. van der Laan, C. Westra, C. Haas, and G. A. Sawatzky, Phys. Rev. B **23**, 4369 (1981).
[30] S. Sugano, Y. Tanabe, and H. Kamimura, *Multiplets of Transition-Metal Ions in Crystals* (Academic, New York, 1970).
[31] J. C. Slater and G. F. Koster, Phys. Rev. **94**, 1498 (1954).
[32] W. A. Harrison, *Electronic Structure and the Properties of Solids* (Freeman, San Francisco, 1980).
[33] P. A. Cox, Struct. Bonding (Berlin) **24**, 59 (1975).
[34] P. S. Bagus, J. L. Freeouf, and D. E. Eastman, Phys. Rev. B **15**, 3661 (1977).
[35] J. S. Griffith, *The Theory of Transition-Metal Ions* (Cambridge University Press, Cambridge, 1964).
[36] J. S. Griffith, *The Irreducible Tensor Method for Molecular Symmetry Groups* (Prentice-Hall, Englewood Cliffs, NJ, 1962).
[37] A. F. Nikiforov, V. B. Uvarov, and Y. L. Levitan, *Tables of Racah Coefficients* (Pergamon, Oxford, 1965).
[38] We note that preliminary calculations in the pseudocubic structure gave essentially the same DOS results. This similarity is reasonable because the rhombohedral distortion in $LaCoO_3$ is not very large; see Ref. 27.
[39] G. Thornton, F. C. Morrison, S. Partington, B. C. Tofield, and D. E. Williams, J. Phys. C **21**, 2871 (1988).
[40] The band gap estimated from spectroscopic results is approximately 0.9 eV; see Ref. 4.
[41] The self-interaction-corrected density-functional formalism provides a much better estimate of the magnitude of the band gaps in transition-metal oxides. See, for instance, A. Svane and O. Gunarsson, Phys. Rev. Lett. **65**, 1148 (1990).

[42]The band gap of $LiCoO_2$ given by the band-structure calculation is 1.2 eV while the optical band gap determined by spectroscopic methods is 2.7 eV; see Ref. 26.

[43]J. J. Yeh and I. Lindau, At. Data Nucl. Data Tables **32**, 1 (1985).

[44]*Unoccupied Electronic States,* edited by J. C. Fuggle and J. E. Inglesfield (Springer, Berlin, 1992).

[45]The La $4f$ bands do not contribute to the O $1s$ x-ray absorption spectrum because the O $2p$–La $4f$ hybridization is negligible.

[46]M. Grioni, J. F. van Acker, M. T. Czyzyk, and J. C. Fuggle, Phys. Rev. B **45**, 3309 (1992).

[47]J. J. M. Michiels, M. Grioni, and J. C. Fuggle, J. Phys. Condens. Matter **4**, 6943 (1992).

[48]To compare the relative stability of the low-spin and high-spin state it is completely necessary to consider also the off-diagonal electrostatic interactions. These interacations alone stabilize the low-spin state by approximately 1.2 eV by mixing the $t_{2g}^6(^1A_1)$ and the $t_{2g}^4e_g^2(^1A_1)$ states.

[49]J. van Elp, J. L. Wieland, H. Eskes, P. Kuiper, G. A. Sawatzky, F. M. F. de Groot, and T. S. Turner, Phys. Rev. B **44**, 6090 (1991).

[50]A. E. Bocquet, T. Mizokawa, T. Saitoh, H. Namatame, and A. Fujimori, Phys. Rev. B **46**, 3771 (1992).

[51]A. Fujimori, A. E. Bocquet, T. Saitoh, and T. Mizokawa, J. Electron Spectrosc. Relat. Phenom. **62**, 141 (1993).

[52]J. Zaanen, G. A. Sawatzky, and J. W. Allen, Phys. Rev. Lett. **55**, 418 (1985).

[53]M. Abbate, F. M. F. de Groot, J. C. Fuggle, A. Fujimori, Y. Tokura, Y. Fujishima, O. Strebel, M. Domke, G. Kaindl, J. van Elp, B. T. Thole, G. A. Sawatzky, M. Sacchi, and N. Tsuda, Phys. Rev. B **44**, 5419 (1991).

[54]M. Abbate, F. M. F. de Groot, J. C. Fuggle, A. Fujimori, O. Strebel, F. Lopez, M. Domke, G. Kaindl, G. A. Sawatzky, M. Takano, Y. Takeda, H. Eisaki, and S. Uchida, Phys. Rev. B **46**, 4511 (1992).

[55]J. van Elp *et al.* (unpublished).